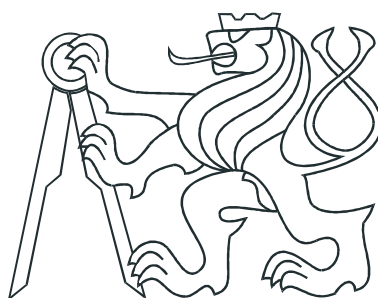


CZECH TECHNICAL UNIVERSITY IN  
PRAGUE

Faculty of Nuclear Sciences and Physical  
Engineering

Department of Physics



## Research project

Luminosity determination at LHC

**Bc. Jan Půček**

**Supervisor: doc. Jesús Guillermo Contreras Nuño, PhD.**

**Prague, 2018**

ČESKÉ VYSOKÉ UČENÍ TECHNICKÉ  
V PRAZE

Fakulta Jaderná a Fyzikálně Inženýrská

Katedra Fyziky



## Výzkumný úkol

Stanovení luminozity na LHC

Bc. Jan Půček

Školitel: doc. Jesús Guillermo Contreras Nuño, PhD.

Praha, 2018



Katedra: fyziky

Akademický rok: 2017/2018

## VÝZKUMNÝ ÚKOL

**Student:** Jan Půček

**Studijní program:** Aplikace přírodních věd

**Obor:** Experimentální jaderná a částicová fyzika

**Vedoucí úkolu:** doc. Guillermo Contreras Nuno, Ph.D.

**Název úkolu (česky/anglicky):** Stanovení luminozity na LHC/Luminosity determination at LHC

### **Pokyny pro vypracování:**

1. Zpracujte rešerši těchto témat:
  - a) Luminozita a metody jejího stanovení
  - b) Měření luminozity na LHC
2. Simulujte luminozitu pomocí modelu dvojné Gaussovy distribuce
3. Simulujte luminozitu pomocí metody primárního vertexu

Součástí zadání výzkumného úkolu je jeho uložení na webové stránky katedry fyziky.  
Práce bude vypracována v anglickém jazyce.

### **Literatura:**

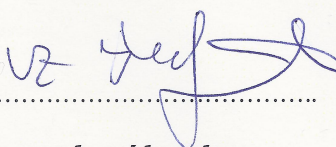
[1] T. Lhc. collaboration, „Precision luminosity measurements at LHCb“, Journal of Instrumentation, roč. 9, č. 12, s. P12005–P12005, pro. 2014 [Online]. Available: <http://dx.doi.org/10.1088/1748-0221/9/12/P12005>

[2] ATLAS Collaboration, „Luminosity determination in pp collisions at  $\sqrt{s} = 8$  TeV using the ATLAS detector at the LHC“, The European Physical Journal C, roč. 76, č. 12, lis. 2016 [Online]. Available: <http://dx.doi.org/10.1140/epjc/s10052-016-4466-1>

[3] P. Grafstrom a W.Kozanecki, Luminosity determination at proton colliders, Prog. Part. Nucl. Phys. 81 (2015) 97-148

**Datum zadání:** 27.10.2017

**Datum odevzdání:** 30.06.2018

  
.....  
**vedoucí katedry**

**Prohlášení:**

Prohlašuji, že jsem svůj výzkumný úkol vypracoval samostatně a použil jsem pouze podklady ( literaturu, software, atd. ) uvedené v příloženém seznamu.

Nemám závažný důvod proti užití tohoto školního díla ve smyslu § 60 Zákona č. 121/2000 Sb., o právu autorském, o právech souvisejících s právem autorským a o změně některých zákonů ( autorský zákon ).

V Praze dne 20.9.2018

Jan Půček

*Název práce:*

**Stanovení luminozity na LHC**

*Autor:* Jan Půček

*Obor:* Experimentální jaderná a částicová fyzika

*Druh práce:* Výzkumný úkol

*Vedoucí práce:* doc. Jesús Guillermo Contreras Nuño, PhD., Katedra fyziky, Fakulta jaderná a fyzikálně inženýrská, České vysoké učení technické v Praze

---

*Abstrakt:* Tento výzkumný úkol je zaměřen na téma faktorizovatelnosti svazku při van der Meer skenu. Nejprve je uvedena luminozita a relace potřebné k jejímu určení při různých podmínkách srážek. Následně je vysvětlena metoda určení luminozity van der Meer sken. Dále jsou diskutovány implementace této metody na jednotlivých experimentech na LHC a jsou případně doplněny o komplementární metody měření luminozity. V praktické části jsou porovnány výsledky simulace a analytických výpočtů, čímž je stanovena chyba simulace. Jedním z výsledků simulace je zobrazení průběhu funkce zobrazující poměr skutečné luminozity a luminozity stanovené pomocí vdM skenu. Nakonec jsou do simulace zakomponovány detektorové jevy k odhalení případných změn parametrů luminozitního regionu.

*Klíčová slova:* Luminozita, LHC, vdM kalibrace, Detektorové rozmazání

*Title:*

**Luminosity determination at LHC**

*Author:* Jan Půček

*Supervisor:* doc. Jesús Guillermo Contreras Nuño, PhD.

---

*Abstract:* This research project is focused on the topic of bunch factorisation during van der Meer scan. First, luminosity is presented along with relations needed to determine luminosity during different collision conditions. Afterwards a luminosity determination method is explained – the van der Meer (vdM) scan. Next, implementations at the LHC experiments of this method are discussed and occasionally complementary luminosity measurement methods are mentioned. The practical part of this work compares the results of a simulation with analytical calculations, which enables to determine the uncertainty of the simulation. One of the simulation results is a plot showing ratio of true and vdM luminosity. Last, the detector smearing is added into the simulation to reveal an eventual change in parameters of the luminosity region.

*Key words:* Luminosity, LHC, vdM calibration, Detector smearing

## **Acknowledgement**

I want to thank my supervisor, doc. Jesus Guillermo Contreras Nuno Ph.D., for his great mentoring!

# Contents

<b>1</b>	<b>Introduction</b>	<b>11</b>
<b>2</b>	<b>Luminosity</b>	<b>12</b>
<b>3</b>	<b>Van der Meer scan - 22.8.</b>	<b>15</b>
3.1	Theory . . . . .	15
3.2	Corrections . . . . .	17
<b>4</b>	<b>Luminosity determination at the LHC</b>	<b>19</b>
4.1	CMS . . . . .	20
4.2	ALICE . . . . .	22
4.3	ATLAS . . . . .	23
4.4	LHCb . . . . .	25
<b>5</b>	<b>Simulation of luminosity</b>	<b>27</b>
5.1	Benchmarking . . . . .	27
5.2	Simulation uncertainties . . . . .	31
5.3	Bunch non-factorisation . . . . .	34
<b>6</b>	<b>Simulation with a realistic vertex resolution</b>	<b>38</b>
6.1	Vertex reconstruction . . . . .	38
6.2	Detector effects . . . . .	39
<b>7</b>	<b>Conclusion</b>	<b>43</b>

# List of Figures

2.1	Angle correction factor for $\sigma_z = 5$ cm and $\sigma_x = 50$ $\mu\text{m}$ . . . . .	13
2.2	Sketch for the case where the bunches collide under the angle $\Phi$ and are shifted by $\Delta y$ . Taken from [1]. . . . .	14
3.1	Rate of interaction measurement is for each x-separation represented by a black point, which are fitted by a red function (here Gaussian). The fit is integrated to obtain the area under the curve which is equal to the integrated rate needed in luminosity determination Eq. (3.7). . . . .	17
3.2	Deformation of axis during vdM scan with constant drift velocity. Taken from [1]. . . . .	18
4.1	The CMS experiment in a 3D computer model, taken from [2]. . . . .	20
4.2	The ALICE in a 3D computer model, taken from [3]. . . . .	22
4.3	The ATLAS experiment in a 3D computer model, taken from [4]. . . . .	23
4.4	The LHCb experiment in a sketch, taken from [5]. . . . .	25
5.1	Comparison of computed luminosity to analytically predicted luminosity, dependent on the product of the bunch widths in x and y. . . . .	29
5.2	Dependence of luminosity on collision angle. The bunch parameters were: $\sigma_{x,y} = 0.1$ , $\sigma_z = 5.0$ – both bunches had the same widths. The simulation corresponds to the analytical model with an uncertainty of 1%. . . . .	29
5.3	Simulated vdM scan to verify the analytically predicted behavior. . . . .	30
5.4	Simulation output showing the results for the vdM scan in the y-direction while maintaining the crossing angle. This is the last benchmark using single Gaussian bunch profiles to obtain the simulation uncertainty. . . . .	31
5.6	Histogram created from the z-values of Fig.5.5. Values are fitted by a Gaussian function to obtain the uncertainty of the simulation. . . . .	33
5.5	Benchmarking simulation for Double Gaussian bunch profiles. The z-axis/palette represents the ratio of the simulated luminosity divided by the analytically predicted luminosity. . . . .	33

5.7	Dependence of luminosity on correlation factor $\rho$ . The parameters used for the simulation: $\sigma_{x1} = \sigma_{x2} = \sigma_{y1} = \sigma_{y2} = 0.2$ , $\rho_1 = \rho$ , $\rho_2 = 0.5$ . Red line represents analytically computed luminosity and therefore is not a fit! . . . . .	35
5.8	Simulation output demonstrating the x-scan of vdM calibration. There are 25 scan points (black) fitted by a Gaussian function (red). . . . .	35
5.9	Simulation output demonstrating the y-scan of vdM calibration. There are 25 scan points (black) fitted by a Gaussian function (red). . . . .	36
5.10	Non-factorisation ratio computed analytically (red line) and obtained by a simulation (black dots). The simulation results agree with the analytical prediction within the error. . . . .	37
6.1	Dependence of the resolution on the vertex position in the x-direction. For the most part the resolution $\sigma_x$ is around $20\mu m$ , which is comparable to the bunch width. . . . .	40
6.2	Dependence of the resolution on the vertex position in the y-direction. For the most part the resolution $\sigma_y$ is around $20\mu m$ , which is comparable to the bunch width. . . . .	40
6.3	Dependence of the resolution on the vertex position in the z-direction. For the most part the resolution $\sigma_x$ is around $30\mu m$ , which is three orders of magnitude smaller than the bunch width. . . . .	41
6.4	Histogram of generated vertices before smearing, fitted by a 2D Gaussian. The obtained correlation is one fit error away from 0, which is not considered conclusive. . . . .	41
6.5	Histogram of smeared vertices from Fig.6.4. The axes have a different scale. The fit output indicates a non-zero correlation factor. This result confirms the need for further research. . . . .	42

# Chapter 1

## Introduction

This research project covers the topic of luminosity determination at the LHC. First, in Chapter 2 the term luminosity at particle colliders is defined and several mathematical results from the outlined theory are presented. This formalism is further developed in Chapter 3, where a method of absolute luminosity calibration is presented – the van der Meer scan (vdM scan for short). The vdM scan is commonly used across all LHC experiments, however, several experiments have developed a complementary methods for luminosity determination. An overview of the methods is presented in Chapter 4. This chapter closes the theoretical part of the research project. The simulation of bunch overlaps follows and can be found in Chapter 5. This simulation is compared to an analytical computation, which serve as a benchmark of the simulation and to assign to it an uncertainty. The goal of the chapter is to present the non-factorisation ratio – the ratio of the true luminosity to the luminosity computed under the assumption of factorisation – and demonstrate its dependence for different bunch parameters. The Chapter 6 is focused mainly on presenting reconstruction algorithms used at ALICE and detector effects are added into the simulation.

This research project continues the work done in [6]. Which means that several details are omitted to prevent repetition of ideas already presented, but key parts of theory are included to ease the understanding of the practical part – simulation.

The main advances made in the practical part with respect to the results presented in [6] consist of adding the third dimension into the simulation, adding the functionality to treat the case of a crossing angle and adding the possibility to smear generated data to simulate detector effects. The simulation code has been fully rewritten and made more robust, enabling better control, as well as faster and easier creation of desired scripts.

## Chapter 2

# Luminosity

Luminosity is a physical quantity, which relates the rate and the cross section of any process. Once the luminosity is determined for one process it can be used for other processes measured in the same set of collisions. This chapter will introduce several methods of luminosity determination with deeper focus on the method of van der Meer (vdM) scans, which is further analysed in the next chapter. The theory is needed for comparing with the simulation (more on this topic in Chapter 5), so one can rely on its results. Derivations of all presented equations can be found in [6].

The defining equation, where rate  $R$ , cross section  $\sigma$  and luminosity  $L$  are related, is Eq. (2.1).

$$R = L\sigma. \quad (2.1)$$

Luminosity is the proportional factor between rate and cross section. Furthermore one can derive Eq. (2.2), which involves two processes (A and B) and shows one of the first methods of measuring cross sections for different processes.

$$\frac{R_A}{\sigma_A} = \frac{R_B}{\sigma_B}. \quad (2.2)$$

For colliders with bunched beams, it is possible to relate luminosity with the accelerator's parameters as shown in Eq. (2.3), where  $K$  is a kinematic factor,  $n_b$  is the number of bunches,  $f$  is the revolution frequency,  $N_{1,2}$  is the number of particles in the two colliding bunches and most importantly  $S_{1,2}$  which is the bunch probability distribution.

$$L = Kn_b f N_1 N_2 \int_{-\infty}^{\infty} S_1(x, y, z, t) S_2(x, y, z, t) dx dy dz dt. \quad (2.3)$$

This equation works only for head-on collisions. Other collision possibilities are collisions under a crossing angle or collisions with an offset. It is common to adapt the equation for Gaussian distribution function, which is a fairly good description of the bunches' actual distribution (for the case of LHC bunches).

The following equations present the luminosity formulas for Gaussian bunches, which both have the same variance in each direction ( $\sigma_x, \sigma_y, \sigma_z$ ). For head-on collisions luminosity is computed by Eq. (2.4). A great property of Gaussian distribution is that the offset can be factorised, which results into a product of head-on term with a coefficient as shown in Eq. (2.5).

$$L_{HeadOn} = \frac{n_b f N_1 N_2}{4\pi(\sigma_x \sigma_y)} \quad (2.4)$$

$$L_{Offset} = L_{HeadOn} C_{Offset}, \quad C_{Offset} = \exp\left(-\frac{(\Delta x)^2}{4\sigma_x^2}\right) \exp\left(-\frac{(\Delta y)^2}{4\sigma_y^2}\right) \quad (2.5)$$

For collisions with crossing angle  $\phi$  it will be assumed that  $\phi$  is small and the angle denotes a tilt of the bunches in the x-z plane. Under these assumptions it is possible to calculate the luminosity for collisions under a crossing angle, see Eq. (2.6).

$$L_{Angle} = L_{HeadOn} C_{Angle}, \quad C_{Angle} = \frac{1}{\sqrt{1 + \left(\frac{\theta \sigma_z}{2\sigma_x}\right)^2}} \quad (2.6)$$

Figure 2.1 shows a representative example of the correction factor for different angles. For an angle of  $500 \mu\text{rad}$  the luminosity decreases by more than 10% for bunch dimensions close to those used at the LHC.

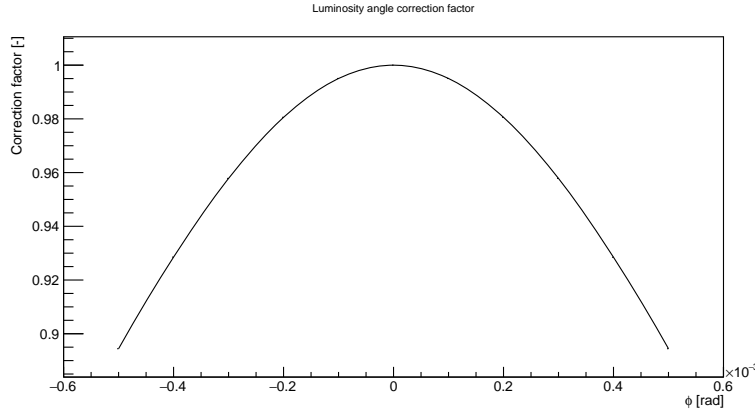


Figure 2.1: Angle correction factor for  $\sigma_z = 5 \text{ cm}$  and  $\sigma_x = 50 \mu\text{m}$ .

Both phenomena (crossing angle, offset) decrease the luminosity, which is actually used in experiments like ALICE, which needs lower collision rate compared to ATLAS. However, the crossing angle is not used only to decrease the luminosity, but mainly to avoid satellite collisions. This type of collision is unwanted as they clog the detector and take place in unwanted locations. Satellite

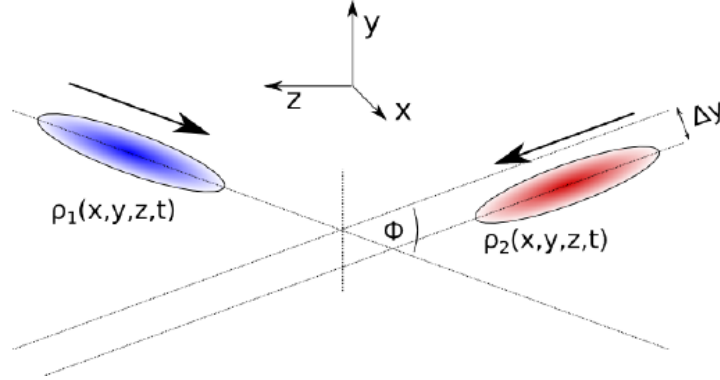


Figure 2.2: Sketch for the case where the bunches collide under the angle  $\Phi$  and are shifted by  $\Delta y$ . Taken from [1].

collisions are the ones, where a bunch collides with a particle in an overfilled bucket.

A case, which is used rarely is beam offset while maintaining non-zero crossing angle. The source of the solution is [1, p. 26]. The sketch of the situation is shown in Fig.2.2. The Eq. (2.7) gives the non-trivial expression for luminosity under the conditions stated above.

$$L_{Off+Angle} = L_{HeadOn} C_{Offset} C_{CrossingAngle} \exp\left(\frac{B^2}{A}\right) \quad (2.7)$$

$$A = \frac{\sin^2 \Theta}{\sigma_y^2} + \frac{\cos^2 \Theta}{\sigma_z^2}, \quad B = \frac{\Delta y \sin \Theta}{2\sigma_y^2}, \quad \Theta = \frac{\Phi}{2}$$

A challenge nowadays is to enhance luminosity, while preserving the same crossing angle. A possible solution to this problem have been crab waist and crab crossing collisions [7, 8] invented in the 1980's. The implementation at LHC (SPS) was successful on 23 May 2018 and it will play a key role in the high luminosity upgrade [9].

The term luminosity has been introduced in this chapter and several theoretical cases of luminosity calculation have been presented. All presented equations will be of use in Chapter 5, where the uncertainties on the numerical simulation will be estimated.

## Chapter 3

# Van der Meer scan - 22.8.

The method [10] pioneered by Simon van der Meer in 1968 is most commonly used today at hadron colliders. Its aim is to calibrate a reference cross section, which is later used during data taking. This chapter will cover in brief the theory of this method and the next chapter will cover the experimental implementation at the LHC experiments.

### 3.1 Theory

The van der Meer scan is based on the movement of beams in two orthogonal directions while measuring the rate of interactions. This enables us to specify a so called visible cross section  $\sigma_{vis}$ , which during data-taking plays the role of a reference cross section and the detectors used during the vdM scans act as luminometre measuring the rate of interactions. From Eq. (2.1) one determines the luminosity. To measure the visible cross section, it is needed to adapt the Eq. (2.3). Because the process is independent of bunch distributions, it will remain in the form of  $S_1(x, y, z)$  and  $S_2(x, y, z)$ . And as the movement is in two orthogonal directions, it will be assumed, that it is already integrated over  $z$ .

The luminosity for bunches with an offset of  $(\Delta x, \Delta y)$  is

$$L_{\text{vdM}}(\Delta x_0, \Delta y_0) = f n_b N_1 N_2 \int_{-\infty}^{\infty} S_{1x}(x) S_{2x}(x + \Delta x_0) dx \int_{-\infty}^{\infty} S_{1y}(y) S_{2y}(y + \Delta y_0) dy. \quad (3.1)$$

As the beams will move in the orthogonal directions separately, one can label the part integrating over  $y$  as constant (for one chosen separation  $\Delta y$ )

$$L_{\text{vdM}}(\Delta x, \Delta y_0) = C_y \int_{-\infty}^{\infty} S_{1x}(x) S_{2x}(x + \Delta x) dx, \quad (3.2)$$

but the luminosity cannot be directly measured – Eq. (2.1) is used to switch luminosity for rate (a measurable quantity).

$$R(\Delta x, \Delta y_0) = \sigma_{vis} C_y \int_{-\infty}^{\infty} S_{1x}(x) S_{2x}(x + \Delta x) dx. \quad (3.3)$$

$$\int_{-\infty}^{\infty} S_{2x}(x + \Delta x) d\Delta x = \int_{-\infty}^{\infty} S_{2x}(x) dx \quad (3.4)$$

In the Eq. (3.3) the visible cross section has been added. It is possible to integrate the equation in  $d\Delta x$  and use an identity Eq. (3.4) to apply the normalisation of bunch distribution ( $\int_{-\infty}^{\infty} S_i(x) dx = 1$ ) to compute the integrated rate

$$\int_{-\infty}^{\infty} R(\Delta x, \Delta y_0) d\Delta x = \sigma_{vis} C_y. \quad (3.5)$$

With this knowledge, it is possible to compute the integral in  $x$  from the Eq. (3.1) in the following manner

$$\int_{-\infty}^{\infty} S_{1x}(x) S_{2x}(x + \Delta x_0) dx = \frac{R(\Delta x_0, \Delta y_0)}{\int_{-\infty}^{\infty} R(\Delta x, \Delta y_0) d\Delta x}. \quad (3.6)$$

This means that once the rate of interactions is measured for different separations, the value of luminosity can be determined as

$$L_{\text{vDM}}(\Delta x_0, \Delta y_0) = f n_b N_1 N_2 \frac{R(\Delta x_0, \Delta y_0)}{\int_{-\infty}^{\infty} R(\Delta x, \Delta y_0) d\Delta x} \frac{R(\Delta x_0, \Delta y_0)}{\int_{-\infty}^{\infty} R(\Delta x_0, \Delta y) d\Delta y}. \quad (3.7)$$

In a simplified case the measured points are plotted into a graph, fitted by an appropriate function, which is integrated to obtain the  $\int_{-\infty}^{\infty} R(\Delta x_0, \Delta y) d\Delta y$  or in  $x$ -direction  $\int_{-\infty}^{\infty} R(\Delta x, \Delta y_0) d\Delta x$ . An illustration of the possible scan outcome is in Fig.3.1.

In a real world scenario the scan outputs need to be corrected for several measurement artifacts (such as orbit drift, length-scale uncertainty, pileup etc.) plus the key assumption which has not been mentioned before is, that the bunch distributions can be factorised into these two orthogonal directions (which is not always true). For these cases a generalisation of the vDM method has been developed which can be found in [11], where luminosity is computed as follows

$$L_{\text{vDM}}(\Delta x_0, \Delta y_0) = f n_b N_1 N_2 \frac{R(\Delta x_0, \Delta y_0)}{\int_{-\infty}^{\infty} R(\Delta x, \Delta y_0) d\Delta x d\Delta y}. \quad (3.8)$$

The great disadvantage of this approach is the high time demand. For this reason it is not used at LHC – although it introduces an uncertainty on luminosity value of around 1.5% at CMS.

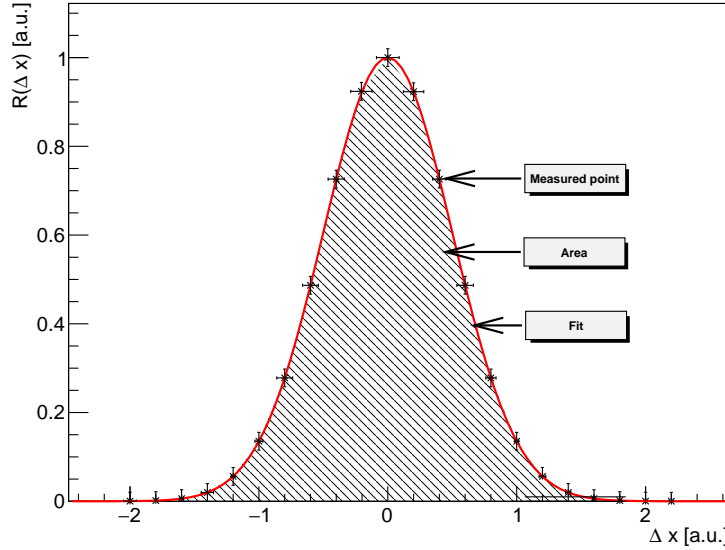


Figure 3.1: Rate of interaction measurement is for each x-separation represented by a black point, which are fitted by a red function (here Gaussian). The fit is integrated to obtain the area under the curve which is equal to the integrated rate needed in luminosity determination Eq. (3.7).

## 3.2 Corrections

In this section several corrections to the vdM scan data will be discussed – correction to the length of the step, correction to the orbit drift and XY-correlations.

First of all, the calibration is done separately for each bunch pairs as the bunch population may change. The results are later combined, however, for the analysis they are treated separately.

During the vdM scan a length-scale calibration is performed, which "calibrates" the beam offset. The goal of this correction is to fine tune the conversion factor between magnet current and the beam displacement. That is why both beams are shifted in the same direction and the centre of the luminosity region is measured. The measured shift is compared with the machine input. A linear fit determines the correction needed. For example in 2015 at CMS the correction factor was 0.983 (0.985) in the horizontal (vertical) direction.

The orbit drift is a more complex problem. It has different effects in the scan plane and in the non-scan (constant) plane. The drift narrows or widens the scan curve in the scan direction, depending on the direction of drift and assuming constant velocity of the drift. In the non-scan plane the effect is different – the

scan behaves as if the axis are tilted (not orthogonal) – see Fig.3.2. However, orbit drifts are difficult to measure precisely, so most of the LHC experiments do not correct for it, only assign a measurement uncertainty.

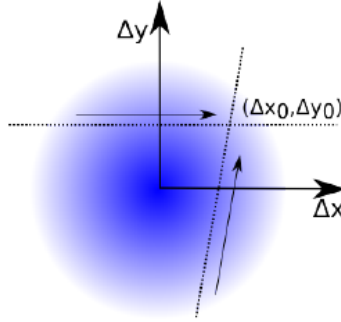


Figure 3.2: Deformation of axis during vdM scan with constant drift velocity. Taken from [1].

As described earlier, in general one cannot assume factorisable bunches. The effect of non-factorisation has been studied in [6], where it is estimated, that the correction can be as high as 3% – depending on the correlation factor in the bunches. To measure the correction, primary vertices are reconstructed and fitted by appropriate bunch distributions – different for each bunch crossing. Then the correction factor is extracted from the fit parameters. More on this topic can be found in Chapter 5.

This chapter has given a brief overview of the van der Meer scan method. With the main focus of this work on the LHC, more information about implementing this method will be demonstrated in the next chapter.

## Chapter 4

# Luminosity determination at the LHC

There are four main experiments at the LHC, each having a different research goal. Due to the focus on different aspects of particle collisions the detectors and methods of obtaining data vary. However, all four experiments use the vdM scan to calibrate absolute luminosity. The difference is in the experimental setup and application of corrections. The best precision of the luminosity measurement on a bunched hadron collider is 1.16% determined by LHCb (year 2014, [12]). This chapter will briefly introduce each experiment, give a description of the detectors used to measure the luminosity and present the experimental setup of vdM scans. The last paragraph in each section will be devoted to methods used/developed on the experiment for the purpose of lowering the luminosity uncertainty.

One common measurement is done for every experiment at the LHC and that is bunch population measurement, which appears in Eq. (2.3) under the  $n_{1,2}$ . To measure the bunch population several special devices have been developed at the LHC. A DC current transformer (DCCT), a device based on the flux-gate magnetometer principle, measures the total beam population – meaning it cannot distinguish between bunches. Its resolution and range are astonishing having  $1\mu A$  as rms for 1s average and a range from  $8\mu A$  to  $860mA$ . To measure the bunch-by-bunch population a Fast Beam Current Transformer is used. It cannot measure absolute values of bunch population, but only relative. However, it is capable of measuring all 3564 nominal bunches with 25ns slots. In order to assign absolute values, the fractions are multiplied by the value obtained by the DCCT. At the LHC there are two DCCTs and two FBCT per beampipe [13, 14].

## 4.1 CMS

The Compact Muon Solenoid Experiment (CMS) is the heaviest of all experiments weighting over 14000 tonnes. Its goal is to search for new particles, gravitons or even supersymmetric particles or new phenomena such as micro black holes and new states of matter such as quark-gluon plasma [15]. An overview of the whole experiment is on Fig.4.1, where several of its parts are described.

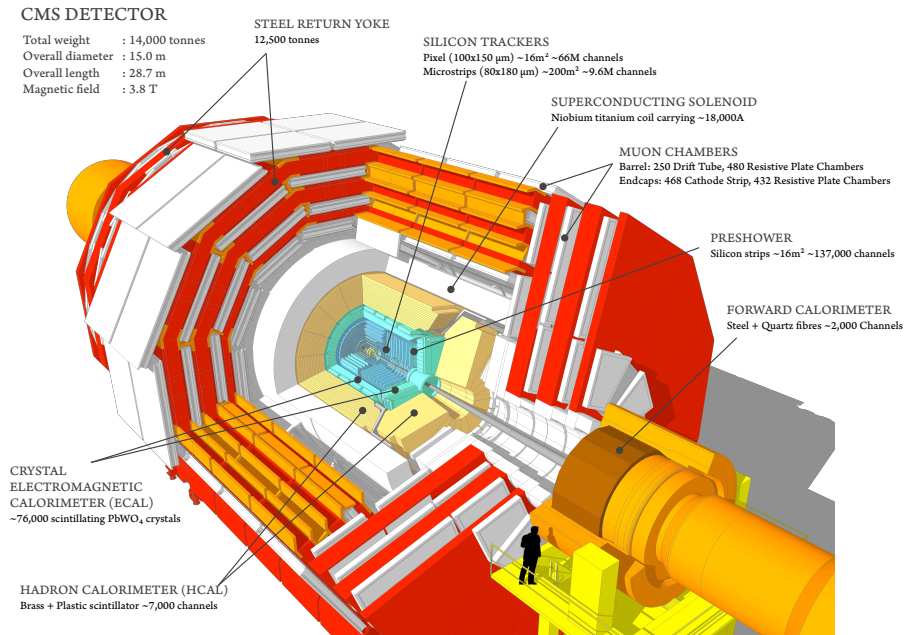


Figure 4.1: The CMS experiment in a 3D computer model, taken from [2].

The detectors that monitor luminosity at CMS are: the Pixel Luminosity Telescope (PLT), the Fast Beam Condition Monitor (BCM1f) and the Forward Hadronic Calorimeter (HF). All three have fast readout asynchronous to the whole CMS apparatus, each independent of the other two. This provides three independent sources of luminosity measurement. The CMS uses the so-called Pixel Cluster Counting method to measure luminosity offline, which uses the central barrel, made of silicon pixel detectors. The silicon pixel detectors make up the PLT as well, where the PLT is used during emittance scans.

First, a clarification of the methods used to measure luminosity will be given. During physics runs, CMS monitors the "online" luminosity by PLT, BCM1f and HF. These detectors give the instantaneous luminosity. When all the data is collected the offline method is engaged to obtain the integrated luminosity

(during the whole data taking). The PCC is an offline method which counts clusters to compute the luminosity as can be seen from Eq. (4.1), where  $f$  is the revolution frequency. The  $\sigma_{vis}^{PCC}$  is the cross section calibrated during the vdM scan.

$$L = \frac{\langle N_{clusters} \rangle f}{\sigma_{vis}^{PCC}} \quad (4.1)$$

The exact implementation of the vdM scans at CMS in 2015 employed 30 pp bunches colliding with no crossing angle. The scan sequence included 2XY scans followed by a length-scale calibration (LSC), Beam Imaging, another LSC and finished by 1XY scan. The XY scans consisted of 25 steps in each direction, each step measured for 30 seconds. In the XY scan both beams move across one another and the maximal offset is  $\pm 6\sigma_b - 6$  standard deviations of the beam width. The Beam Imaging scan included only 19 steps, where one beam was fixed and the other was being moved. The offset limits were set to  $\pm 4.5\sigma_b$ . [16]

A special method has been developed at CMS to evaluate the linearity and stability of BRIL (PLT+BCM1f+HF), plus it gives  $\sigma_{vis}$  for each fill. The method is called Emittance scan and it is performed at the beginning and end of each fill. The Emittance scan measures 7 steps in each direction, staying for 10 seconds on each step. Between the change of direction head-on collisions are measured for 5 seconds. As the scans are short, the results are fitted by a single Gaussian distribution to obtain beam widths. [17]

## 4.2 ALICE

A Large Ion Collider Experiment (ALICE) is optimized for heavy ion collisions, which means that the 19 sub-detectors have to track and identify the tens of thousands of particles produced in each collision. The research goal of this experiment is to study matter heated to 10000 times the temperature of the Sun and to answer why protons and neutrons weight more than 100 times more than the quarks they are made of [18]. An overview of the whole experiment with labels of all subsystems is shown in Fig.4.2.

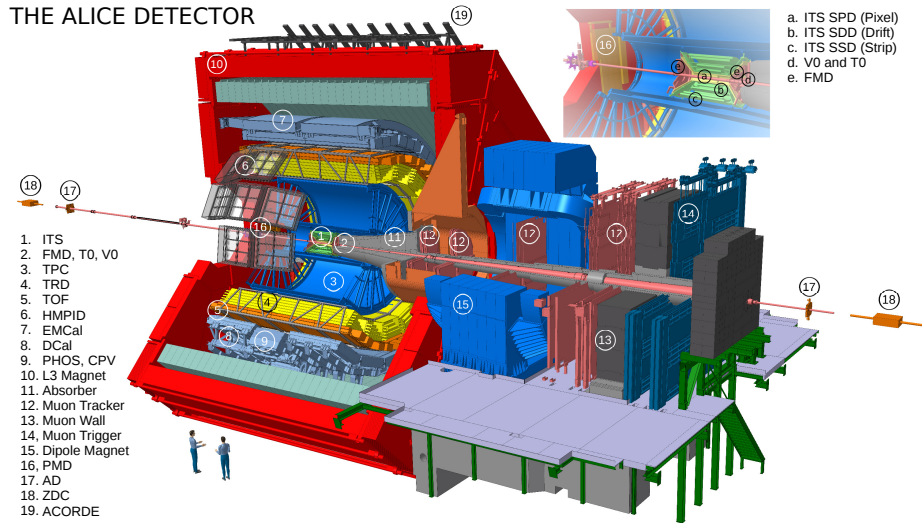


Figure 4.2: The ALICE in a 3D computer model, taken from [3].

ALICE uses two detectors, which serve as luminometers. Both detectors have two parts which are located at both sides of the interaction point. The V0 has parts A and C, each consists of 32 scintillator tiles. V0-A is 340 cm from the nominal interaction point (IP) and V0-C is 90 cm from the IP along the beam axis. The detector T0 has as well parts A and C, each being an array of 12 Cherenkov counters. T0-A is 370 cm from the IP and T0-C is 70 cm from the IP (one is behind the V0-A and the second is in front of the V0-C). Both V0 and T0 have great time resolution and thus serve as triggers for the other sub-detectors.

Methodology that has been used during the 2013 p-Pb (Pb-p) vdM scan will be presented. Due to the asymmetric setup of luminometers and the shift of the center-of-mass frame, the vdM scan had to be done for both configurations. The boundaries for beam movement have been set as  $\pm 6\sigma_b$ . The vdM scan consists of 2 repeated scans, each including a 2 X and Y scans. The first XY scan was

made in horizontal direction and then in the vertical, while shifting the beam from negative to positive. The second XY scan was the same as the first one except the shifting, which was done from positive to negative. The scan in each direction was measured at 25 points, where every point was measured for 30 seconds [19].

### 4.3 ATLAS

A Toroidal LHC ApparatuS (ATLAS) is the largest experiment at the LHC measuring 46 meters in length and 25 meters in height. Its goal is to study how elementary particles gain mass and shed light upon antimatter behaviour. At ATLAS during data taking as many as 1 billion collisions occur every second [20]. An overview of the whole experiment with labels of subsystems is shown in Fig.4.3.

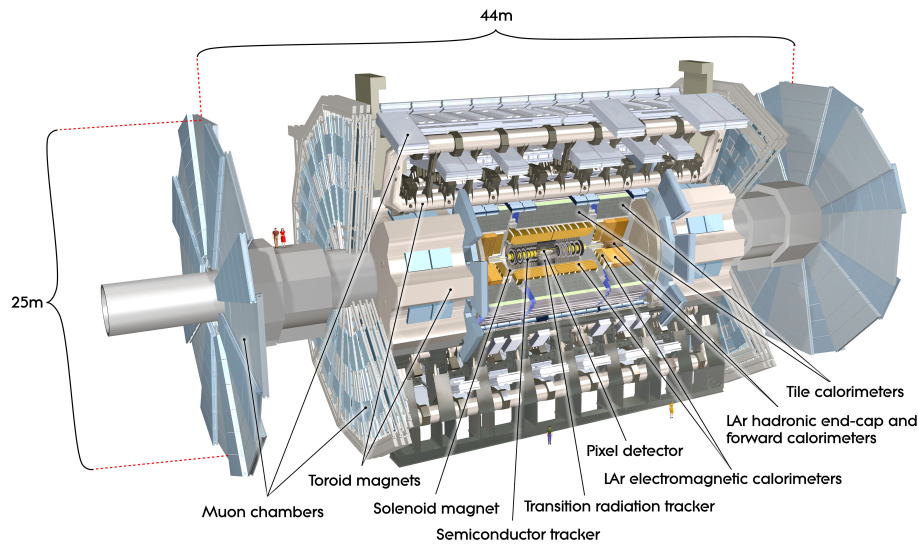


Figure 4.3: The ATLAS experiment in a 3D computer model, taken from [4].

ATLAS uses several detectors and methods to determine luminosity. Two detectors that are capable of delivering online luminosity values are LUCID (Luminosity measurement using a Cherenkov Integrating Detector) and BCM (Beam Conditions Monitor). LUCID consists of 16 aluminium tubes filled with  $C_4F_{10}$  on each side of the IP at a distance of 17 meters. On the other hand BCM is formed by 4 diamond sensors at each side of the IP at a distance of 1.84 meters, where they are divided into 2 parts – vertical and horizontal,

each having its own readout. A Bunch-by-Bunch measurement is possible from the LUCID and the BCM due to their fast electronics, running autonomously from the main DAQ (data acquisition system). Parts of the detector located forward are labelled "A" – BCM-A, LUCID-A and in the backward direction are labelled "C" – BCM-C, LUCID-C. This labelling is important, because A and C detectors are treated as independent devices.

The detectors mentioned above are operated with the EventOR algorithm. The algorithm requires at least one hit anywhere in the detector. With the assumption that the number of interactions obeys a Poisson distribution, the probability of recording such an event is

$$P_{EVENTOR} = \frac{N_{OR}}{N_{BX}} = 1 - e^{-\mu_{vis}^{OR}}, \quad (4.2)$$

where BX represents a bunch crossing and  $\mu_{vis}^{OR}$  is the interaction rate. However, this algorithm can be saturated under the condition that  $\frac{N_{OR}}{N_{BX}} = 1$ . For LUCID\_EventOR the saturation happens after a one-minute interval at 20 interactions per bunch crossing.

The method developed at ATLAS to measure luminosity for the already saved data is based on track counting. This method utilises the inner detectors – Pixel, SCT (silicon micro-strip detector) and TRT (straw-tube transition-radiation detector). Track counting assumes that the luminosity is proportional to the number of charged-particle tracks per bunch-crossing. The reconstruction of tracks uses an inside-out algorithm with a combinatoric Kalman filter. There are several constraints on the event to be accepted. First, there has to be 9 hits in the silicon detector, zero "holes" (pixels which didn't trigger, although a hit is expected). Second, a transverse momentum above 0.9 GeV/c has to be present and lastly a constraint on the impact parameter is given. During a physics run, there may appear fake tracks which have to be corrected.

In 2012 there were several sessions of vdM calibration – in April, July and November. The session in April conserved the physics run setup of the collisions, which resulted in high pile-up rate and thus lower precision. The scans in July and November were similar, both colliding without crossing angle. The scan contained 4 sets of centered XY scan (working point being 0,0) and 2 sets of off-axis scan (work point being 340  $\mu\text{m}$  and 200  $\mu\text{m}$ ). The boundaries, number of steps and time per step were the same as for all other experiments - 25 steps, 30 seconds per step and boundaries  $\pm 6\sigma_b$ . [21]

## 4.4 LHCb

The Large Hadron Collider beauty experiment (LHCb) has highest vertexing resolution to date at the LHC. It is focused on measuring the beauty quark, which determined the design of the detector – the beauty quark is strongly boosted, thus stays close to the beampipe. One of the research goals is to look for anomalies in the CPT symmetry [22]. The overview of the experiment is in Fig.4.4.

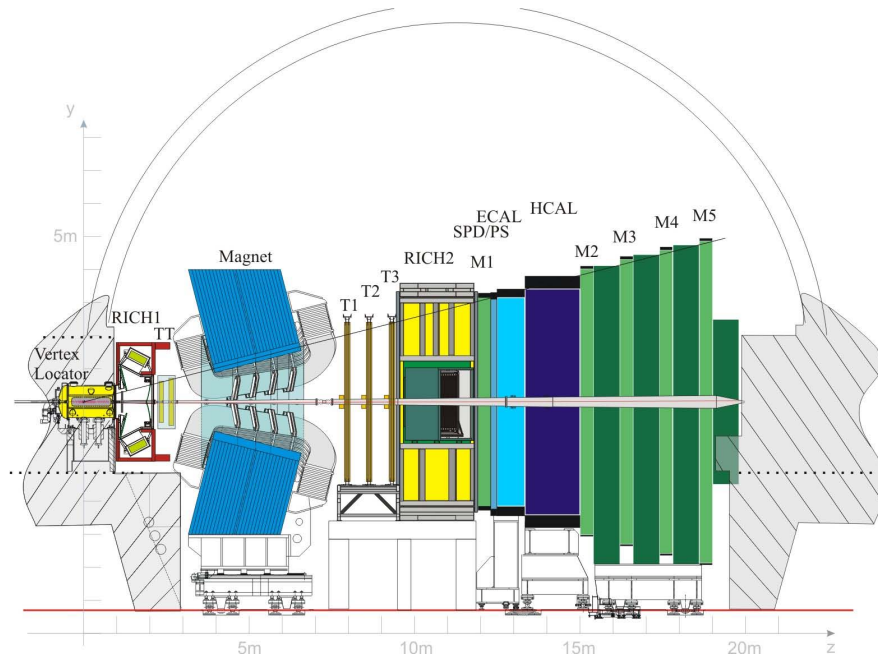


Figure 4.4: The LHCb experiment in a sketch, taken from [5].

The luminosity measurement at the LHCb is based on the VELO (Vertex Locator). It is a detector with 21 layers of radial and azimuthal silicon-strip sensors. The VELO is divided into two halves, which can be retracted from the beam during injection and beam adjustments to a distance of 30 mm from the beam. During stable beam and collisions the halves move closer to the beam to obtain highest possible precision, being only 8.2 mm from the beams.

The method of luminosity determination still uses the vdM scan, but is complemented by and compared to a special method called Beam-Gas Imaging (BGI). The luminosity is measured during physics runs by a special trigger setting, which has a fixed average frequency of 1000 Hz. The rate is divided into several types of "collisions" – 70% is dedicated to beam-beam collisions, 15% is assigned for beam-1 against empty bunch slot, 10% is devoted to collisions

with beam-2 against empty bunch slot and 5% is set for collisions with empty bunch slots in both beams. This setting enables easy background subtraction as well as beam monitoring. The observables used at the LHCb to determine the luminosity are the number of primary vertices (PV), the number of reconstructed tracks in VELO, the number of muons reconstructed in the muon system, the number of hits in the Pile-Up system (PU) and in the Scintillating Pad Detector (SPD), the transverse energy deposited in the calorimeters.

Before a report of the experimental setup for the vdM scan, a description of the BGI method will be given. This method uses vertices to reconstruct the luminosity region and the bunch distributions as well. To measure each bunch distribution a collisions with static atoms of gas were enabled by degrading the vacuum inside the beam pipe. To degrade the vacuum it was sometimes sufficient to shutdown ion pumps, however, a dedicated gas injection system of neon was developed. The reconstruction of events is done offline, as finding primary vertices is a demanding task. There are many selection criteria applied on the measured events. To measure the resolution of vertices, the algorithm "split vertex method" is used. This separates randomly tracks into two subsets, each reconstructing its own vertex. The resolution of vertices is the RMS obtained by fitting histograms of the vertex difference for a specified number of tracks. By obtaining the bunch distributions it is possible to check factorisation, which is impossible to do during a vdM scan.

In 2012 there were 2 vdM scans performed, in April and in July. For this work only the one with pp collisions will be presented. Four XY scans were performed. The beams were always moved symmetrically between the boundaries  $\pm 6\sigma_b$ . The last XY scan in each fill was done with the working point shifted to approximately  $+2\sigma_b$  to cross-check systematic effects. The first and the last scan were rotated with respect to the axes of the LHC. In each fill a LSC is done to verify the beam displacements. The number of steps differs to all other LHC experiments. During the first two scans 31 points were scanned, each measured for 15 seconds per step. The second two scans had only 17 steps in each plane, each step measured for 15 seconds [12].

## Chapter 5

# Simulation of luminosity

To investigate the effects of bunch factorisation in vdM scans and thus inspect the precision of the luminosity determination, a simulation framework has been created. The basic principle is simple – a convolution of two 3D probability distributions creates the so-called luminosity region, which is related to the rate of interaction, measured during real collisions.

In this chapter, the correctness of this method will be discussed (comparison with analytical calculations) and the computation of the simulation uncertainty will be demonstrated. Last but not least, several simulation results will be shown for different initial probability distributions.

The simulation is coded in C++ within the ROOT framework [23]. The idea of the simulation is first to generate random points following a distribution and fill it into a histogram. The histogram represents a bunch, which is later overlapped with another bunch to create a luminosity region. The luminosity region is integrated to obtain the luminosity for that particular collision. Each part of the simulation has to be verified, at least for simple bunch distributions – cases comparable to an analytical computation.

### 5.1 Benchmarking

The goal of benchmarking is to check all parts of the simulation for errors and look for the behaviour which would differ from analytical expectations. The generation of bunches has been verified in [6, p. 41-46]. One remark to be made concerning the  $\sigma$  of 1D cuts made to 2D distribution – there was a bias of 2-4%. This was later resolved – the histogram bins contained low number of entries, which in turn meant lower  $\sigma$  when fitted by the  $\chi^2$  method. Once the likelihood method was used all values were equal to the analytical ones.

The important advantage of the code this year is the addition of the third dimension. So several phenomena were controlled and compared to analytical predictions – luminosity in head-on collisions, effect of a crossing angle ( $y$ - $z$ ), the bunch width determined by a simulated vdM scan and the effect of non-

factorisation (more in section 5.3).

Histograms consist of discrete bins which are filled with entries. This means that the Eq. (2.3) cannot be used with the integral. Instead a sum is used – to get total number of entries summing the complete histogram over all bins is made see Eq. (5.1), where  $N$  is the total number of entries and the distribution is assumed to be normalized. The difference is in the computation of the luminosity region. To get a luminosity region two bunches are overlapped, both having same bin widths in each direction. But to normalise this procedure one has to divide by the bin-widths  $\Delta x$ ,  $\Delta y$ . The reason one does not need to account for  $\Delta z$  is that it is already summed. To obtain a luminosity value from the luminosity region it is sufficient to multiply by the kinematic factor as shown in Eq. (5.2) – the  $n_b$  (number of bunches) and  $f$  (frequency) is set to 1.

$$n \int_{-\infty}^{\infty} S_i(x, y, z) dx dy dz = \sum_{x,y,z=0}^{Nbins} H_i(x, y, z) \quad (5.1)$$

$$Kn_1n_2 \int_{-\infty}^{\infty} S_1(x, y, z + ct)S_2(x, y, z - ct) dx dy dz dt = \sum_{x,y,z=0}^{Nbins} \sum_{i=-Nbinsz}^{Nbinsz} \frac{H_1(x, y, z + i)H_2(x, y, z - i)}{\Delta x \Delta y} \quad (5.2)$$

To be able to compare the simulation (right side of equation 5.2) one must compute the left side, which is already done for head-on collisions with single Gaussian bunch distributions shown in Eq. (2.4). A graph has been made to compare the analytical prediction with the output of the simulation see Fig.5.1. There seems to be a systematic offset of 0.4% and an RMS of 0.1%. In all the following text we will be using an uncertainty of 0.5% arising from the random generation.

To verify correct behavior of the simulation during collisions with crossing angle, the Eq. (2.6) was used. The dependence of the luminosity on the crossing angle was plotted. A fit was done to estimate the simulation uncertainty – the only variable parameter was  $p1$  which is shown in Eq. (5.3). The other parameter which is fixed is the  $p0$  which only represents the fraction  $\frac{\sigma_z}{2\sigma_x}$ . The uncertainty of the  $p1$  is 1%. This was achieved by using the computed value of head-on luminosity instead of the analytical value, which on its own has a 0.5% uncertainty. The result is shown in figure 5.2.

$$\frac{L_{Angle}}{L_{HeadOn}} = \frac{1}{\sqrt{1 + p1 \left( \frac{\theta\sigma_z}{2\sigma_x} \right)^2}} \quad (5.3)$$

Other two checks need to be made, before computing the uncertainties for more complicated cases. One is a vdM scan, which should obey the offset formula Eq. (2.5). To make understanding easier, the ratio of the offset luminosity to the head-on luminosity was plotted and fitted by a Gaussian function.

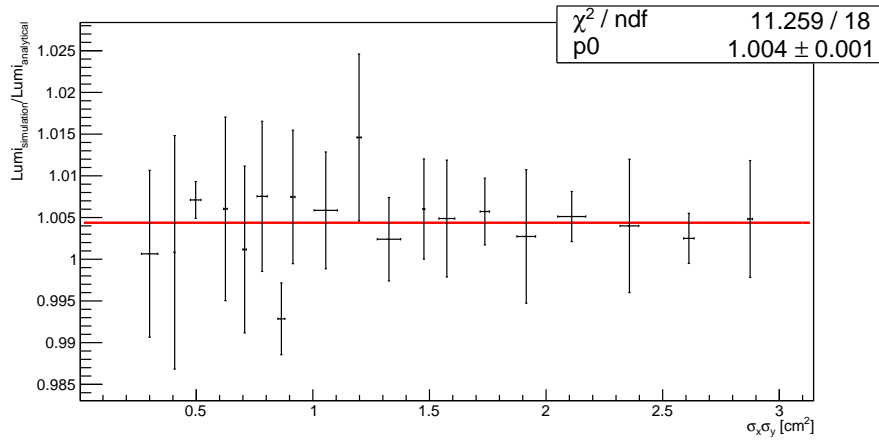


Figure 5.1: Comparison of computed luminosity to analytically predicted luminosity, dependent on the product of the bunch widths in x and y.

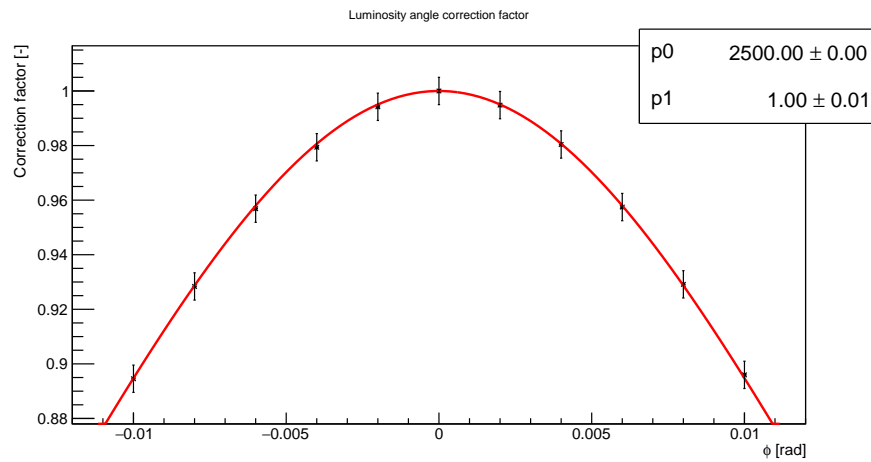


Figure 5.2: Dependence of luminosity on collision angle. The bunch parameters were:  $\sigma_{x,y} = 0.1$ ,  $\sigma_z = 5.0$  – both bunches had the same widths. The simulation corresponds to the analytical model with an uncertainty of 1%.

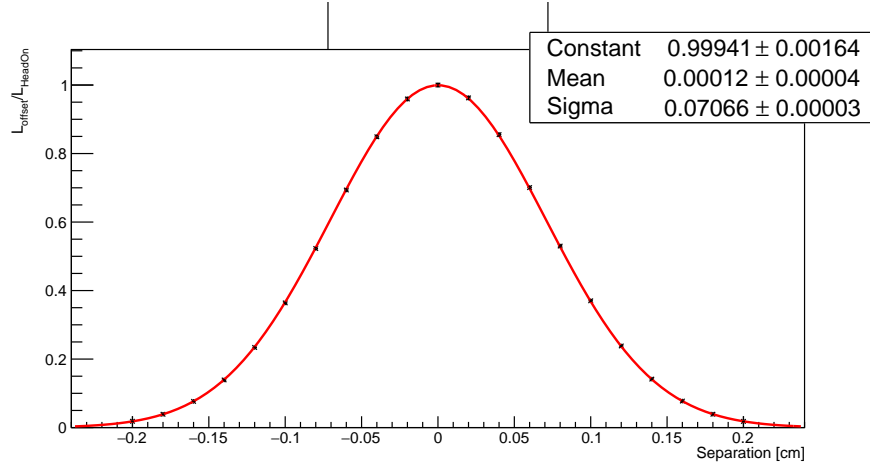


Figure 5.3: Simulated vdM scan to verify the analytically predicted behavior.

The width of the fit  $\sigma_f$  was expected to be  $\sqrt{2}\sigma_{x,y}$  depending on the direction of the offset. For the parameters used in the simulation the expected width was  $\sigma_{f-ex} = 0.07071$  and the one obtained from the simulation was  $\sigma_f = (0.07066 \pm 0.00003)$ . The generated data and fit is in Fig.5.3.

The last verification involves a vdM scan with a crossing angle, because the dependence is more complex, than a multiplication of two correction factors – as was already shown in Eq. (2.7). The correction factor can be rearranged to get Eq. (5.4). For a well visible effect, the common simulation values had to be adjusted –  $\sigma_y = 0.05$ ,  $\sigma_z = 5.2$  and the crossing angle  $\Theta = 0.01$ . The vdM scan should output a Gaussian function with width  $\sigma_{ex} = 0.102021$ . The result of the simulation is in figure 5.4, which reveals the fit value being  $\sigma_f = (0.10238 \pm 0.00009)$ .

$$C = \exp \left[ -\frac{\Delta y^2}{4\sigma_y^2} \left( 1 - \frac{\sigma_z^2 \sin^2 \Theta}{\sigma_z^2 \sin^2 \Theta + \sigma_y^2 \cos^2 \Theta} \right) \right] \quad (5.4)$$

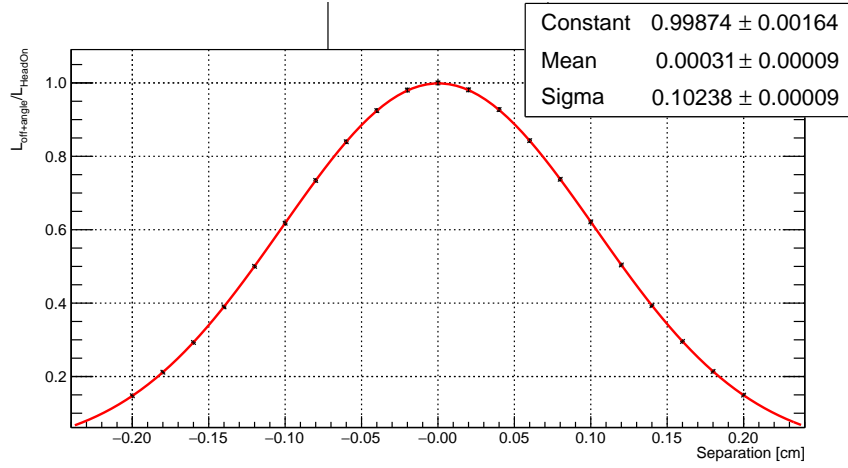


Figure 5.4: Simulation output showing the results for the vdM scan in the y-direction while maintaining the crossing angle. This is the last benchmark using single Gaussian bunch profiles to obtain the simulation uncertainty.

## 5.2 Simulation uncertainties

In this section first the general formula for head-on collisions of Gaussian bunches will be given, which will be useful to evaluate the simulation using double Gaussian bunch profiles. From the benchmarking the uncertainties for a single Gaussian are known. Thus it is possible to estimate the uncertainties for double Gaussian bunches and compare the prediction with the results of a simulation. This will be important for studies presented later in this work to accurately simulate the difference of luminosity determined by a vdM scan and by the simulation.

The most general formula for a head-on luminosity for two colliding Gaussian bunches is in Eq. (5.5) – bunch "1" has widths  $\sigma_{1x,y}$ , bunch two is defined by widths  $\sigma_{2x,y}$ . To understand the usefulness in the case of a double Gaussian bunch profile collisions, it is needed to present the double Gaussian distribution beforehand.

$$L_{\text{HeadOn}} = \frac{n_b f n_1 n_2}{2\pi \sqrt{(\sigma_{1x}^2 + \sigma_{2x}^2)(\sigma_{1y}^2 + \sigma_{2y}^2)}}. \quad (5.5)$$

The double Gaussian distribution is a sum of two single Gaussian distributions with a condition – both single Gaussians have the same mean. In order to leave the distributions normalised the weight factor  $w$  is added as shown in Eq. (5.6), where  $G$  represents a single Gaussian.

$$DG = wG_A + (1 - w)G_B. \quad (5.6)$$

Now to compute the head-on luminosity, the equation will reduce to four parts, each consisting of a single Gaussian part. This way the Eq. (5.5) is used. To make it clear a schematic Eq. (5.7) demonstrates the collision of bunch 1 (consists of Gaussians A and B) with bunch 2 (consists of Gaussians C and D). We want to obtain an estimate of the simulation uncertainty, each integral has a relative error  $\sigma_{rel}$  determined in section 5.1 -  $\sigma_{rel} = 0.5\%$ . This value is used for every integral in Eq. (5.7) and all uncertainties were summed in squares. This fact is expressed in Eq. (5.8), where integrals are noted by subscripts of constituents from Eq. (5.7).

$$L = Kn_1n_2 \int_{-\infty}^{\infty} (W_1G_{1A}G_{2C} + W_2G_{1A}G_{2D} + W_3G_{1B}G_{2C} + W_4G_{1B}G_{2D}) dV dt \quad (5.7)$$

$$\begin{aligned} \sigma_L &= \sigma_{rel} \sqrt{K_1 + K_2 + K_3 + K_4}, & (5.8) \\ K_1 &= (w_1w_21A2C)^2, \\ K_2 &= (w_1(1-w_2)1A2D)^2, \\ K_3 &= ((1-w_1)w_21B2C)^2, \\ K_4 &= ((1-w_1)(1-w_2)1B2D)^2. \end{aligned}$$

The following values are used for the simulation:  $\sigma_{1B-x,y} = 0.5$ ,  $\sigma_{2C-x,y} = 0.3$ ,  $\sigma_{2D-x,y} = 0.5$ ,  $\sigma_{z-1A,2C} = 6.0$ ,  $\sigma_{z-1B,2D} = 5.0$ ,  $\Theta = 0$  and  $w_{1,2} = 0.5$ . The other parameters were varied in the range from 0.2 to 0.7 separately by steps of 0.05. From this knowledge the relative uncertainty calculated by the Eq. (5.8) is around 0.25%. The output is in Fig.5.5, where for the most part the ratio is less than 0.27% away from unity determined from Fig.5.6.

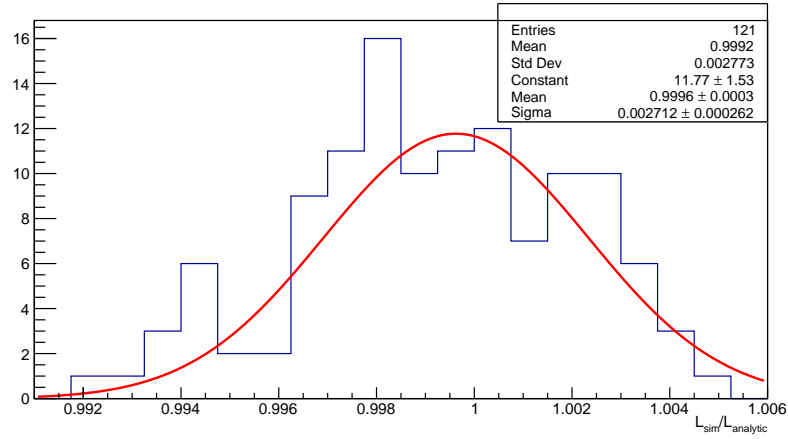


Figure 5.6: Histogram created from the z-values of Fig.5.5. Values are fitted by a Gaussian function to obtain the uncertainty of the simulation.

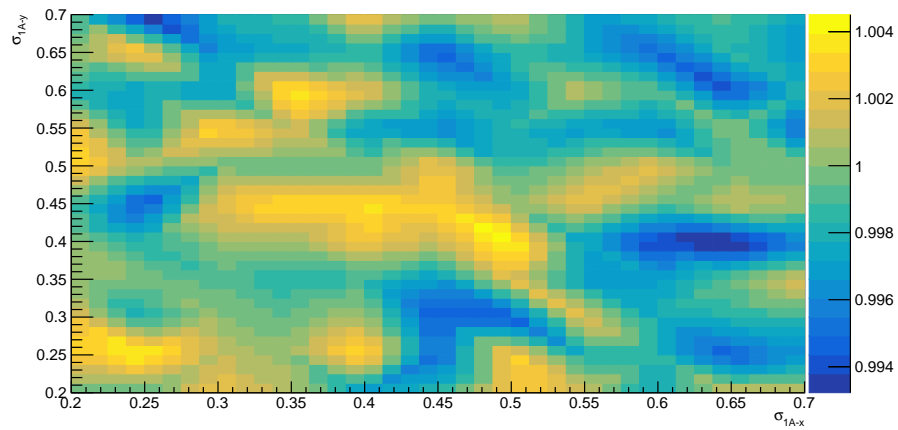


Figure 5.5: Benchmarking simulation for Double Gaussian bunch profiles. The z-axis/palette represents the ratio of the simulated luminosity divided by the analytically predicted luminosity.

### 5.3 Bunch non-factorisation

This section will study the bunch factorisability into two independent directions, which was assumed by Simon van der Meer in his beam height measurement. But during measurements at LHCb (and other experiments) the Beam-Gas Imaging method discovered non-factorisation in the LHC beams. This meant that there had to be a correction applied to the luminosity data obtained by a vdM scan. To compute the correction a quantity has been established –  $R$ , which is not the rate, but the ratio of the luminosity  $L_{true}$ , which would be obtained by grid scan or analytically by **not** factorising into two independent integrals, divided by the luminosity obtained by a vdM scan  $L_{vdM}$ .

In this section the main concern will be to compute analytical correction (mostly taken from [6]) and comparing to a simulated ratio  $R$ . But first a benchmark of the simulation while using correlated bunches will be presented. Then several simulated vdM scans will be compared to analytical predictions. This will enable us to compare the ratio obtained from simulation and from analytical formulas.

The "true" luminosity for head-on collisions with single Gaussian bunches with xy-correlation can be computed from Eq. (5.9)<sup>1</sup>. The value obtained from that formula is "equal" to the value obtained from the simulation as shown in Fig.5.7.

$$L_{true*} = \frac{1}{2\pi\sqrt{\sigma_{x1}^2\sigma_{y1}^2(1-\rho_1^2) + \sigma_{x2}^2\sigma_{y2}^2(1-\rho_2^2) + \sigma_{x1}^2\sigma_{y2}^2 + \sigma_{x2}^2\sigma_{y1}^2 - 2\sigma_{x1}\sigma_{y1}\sigma_{x2}\sigma_{y2}\rho_1\rho_2}} \quad (5.9)$$

To obtain the other part of the ratio  $R$ , the luminosity determined by the vdM  $L_{vdM}$  scan has to be computed. Again taken from [6] the Eq. (5.10) expresses analytically the  $L_{vdM}$ . This is compared to values from simulation, which imitated the vdM scan as described in Chapter 3. The results for various bunch parameters had the maximum difference of 0.7%. Also examples of the simulation output are in Fig.5.8,5.9.

$$L_{vdM*} = 2\pi\sqrt{(\sigma_{x1}^2 + \sigma_{x2}^2)(\sigma_{y1}^2 + \sigma_{y2}^2)}L_{true*}^2 \quad (5.10)$$

<sup>1</sup>Taken from [6], however, a typo occurred in the original computation. Corrected during copying. The star means the constants before integrals are omitted

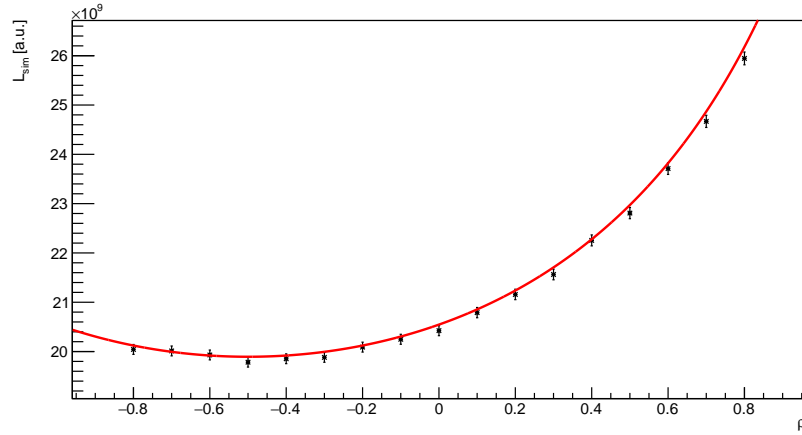


Figure 5.7: Dependence of luminosity on correlation factor  $\rho$ . The parameters used for the simulation:  $\sigma_{x1} = \sigma_{x2} = \sigma_{y1} = \sigma_{y2} = 0.2$ ,  $\rho_1 = \rho$ ,  $\rho_2 = 0.5$ . Red line represents analytically computed luminosity and therefore is not a fit!

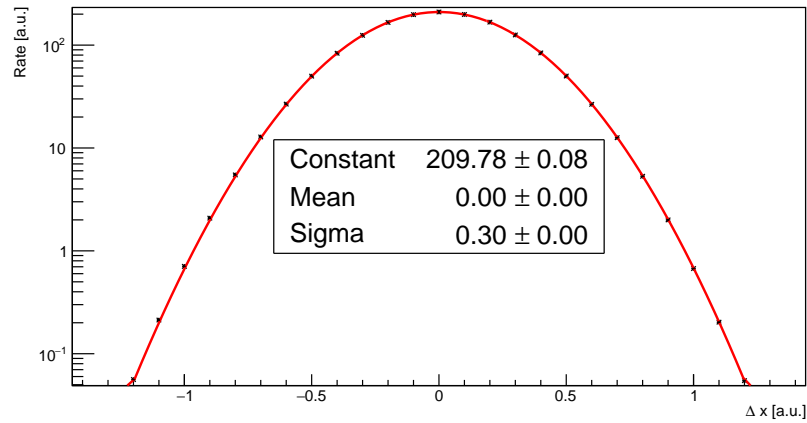


Figure 5.8: Simulation output demonstrating the x-scan of vdM calibration. There are 25 scan points (black) fitted by a Gaussian function (red).

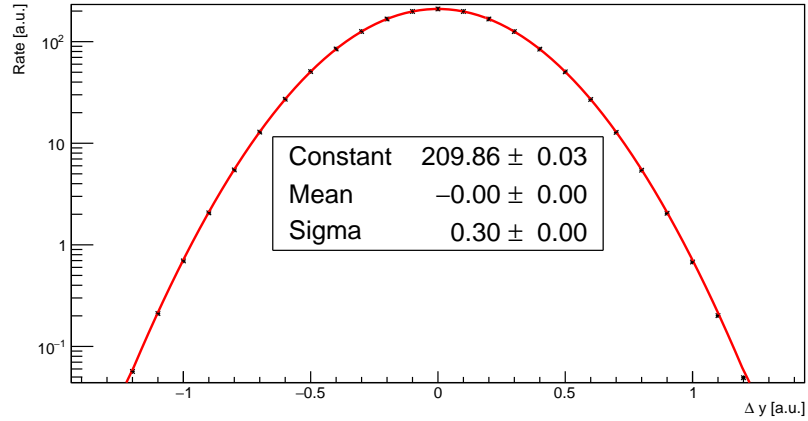


Figure 5.9: Simulation output demonstrating the y-scan of vdM calibration. There are 25 scan points (black) fitted by a Gaussian function (red).

With all this done, it is possible to compare results for the non-factorisation ratio  $R$ . The figure 5.10 compares the pure simulation values (black) with the analytical prediction (red line). The agreement between the results are within the simulation uncertainty. The parameters of the simulation were following:  $\sigma_{x1} = 0.25$ ,  $\sigma_{x2} = 0.2$ ,  $\sigma_{y1} = 0.2$ ,  $\sigma_{y2} = 0.25$ ,  $\rho_2 = 0.3$  and  $\rho_1$  was variable from  $-0.5$  to  $0.5$ .

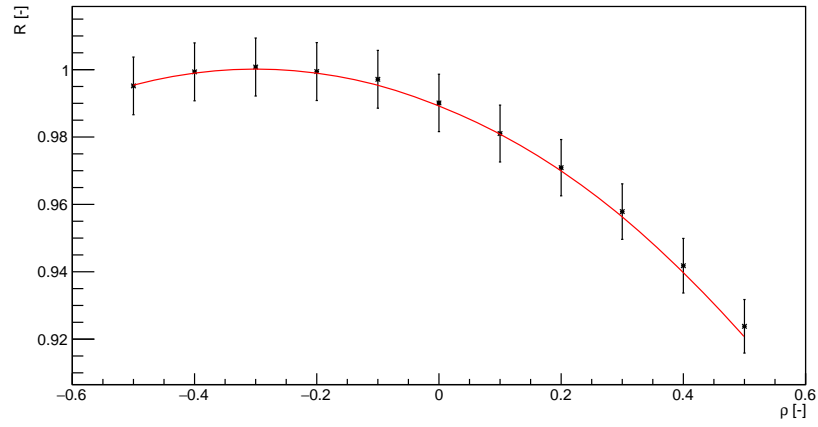


Figure 5.10: Non-factorisation ratio computed analytically (red line) and obtained by a simulation (black dots). The simulation results agree with the analytical prediction within the error.

## Chapter 6

# Simulation with a realistic vertex resolution

The previous chapter demonstrated the difference in the simulation of the measured luminosity compared to the one truly delivered. In this chapter we will mainly focus on the issue of detector smearing, using real-life ALICE data. One of main concerns is, whether the detector smearing can affect the measurement of non-factorisation in the bunches. But before this question is attacked, an introduction to measuring the luminosity region has to be done. The section 6.1 presents the algorithm used at ALICE for reconstructing primary vertices, which make up the luminosity region. The next section 6.2 shows the simulation for smearing using real data, which are also demonstrated.

### 6.1 Vertex reconstruction

The primary vertex is the precise position where a collision took place. This collision generates primary particles. The particles leave a signal inside the detectors, which can be reconstructed into positions in time. All positions of a single particle make up its trajectory in the detector. However, during a collision there may be up to several thousands particles, making it difficult to distinguish them. But this section does not focus on track reconstruction, its main focus is on the vertex finding and vertex fitting algorithms.

The vertex finding algorithm selects tracks, which have the same primary vertex. The goal of the vertex fitting algorithm is to obtain the best fit coordinates of the vertex. The precise method used at ALICE is described in [24]. In short the algorithm minimizes a  $\chi^2$  function, which is a sum over all tracks, "weighted" by the precision of the track. The output is the vertex position and covariance matrix with the uncertainties of the position.

## 6.2 Detector effects

All studies presented in section 5.3 were performed assuming a perfect detector, which had a perfect precision. But is it possible that detector smearing could create or dissolve the non-factorisation effects? For this reason a second part of the simulation has been created. It creates the luminosity region with real-life parameters and then uses gathered data from ALICE to smear the vertices one-by-one, to obtain detector-like data. The further step, which is not yet implemented is to fit the smeared data and compare with the input parameters. In this section the first part is dedicated to analyzing real covariance matrices from the experiment ALICE and the second part compares the luminosity region with and without smearing.

Used data were acquired in pPb collisions with an energy of 8.16 TeV per nucleon pair, the fill number is 5533. After the two XY scans a length-scale calibration was executed. A selection of the data was performed, by picking vertices with more than 15 contributors (this enhances the resolution of the vertex position). The resolution is described by a 3D Gaussian probability distribution. Graphs Fig.6.1, Fig.6.2 and Fig.6.3 display the dependence of the resolution on the vertex position. There are other terms which define the resolution correlations dependent on two coordinates.

The simulation creates a luminosity region, as described in Chapter 5. From the luminosity region a point (representing a vertex) is picked randomly. For each point one resolution covariance matrix is picked (again randomly) and from the distribution, that the covariance matrix represents, is generated one random point which gives the smearing shift of the originally simulated point. Both points and the covariance matrix are saved for further analysis.

To mimic the data the input parameters were set according to a fit done by Christoph Mayer from the ALICE Collaboration<sup>1</sup>. The parameters used are reported in Eq. (6.1).

$$\begin{aligned}
 w_1 &= 0.64 & w_2 &= 0.44 & (6.1) \\
 \sigma_{x1a} &= 36.6 \mu m & \sigma_{x1b} &= 22.0 \mu m & \sigma_{x2a} &= 39.7 \mu m & \sigma_{x2b} &= 37.3 \mu m \\
 \sigma_{y1a} &= 23.5 \mu m & \sigma_{y1b} &= 13.6 \mu m & \sigma_{y2a} &= 26.5 \mu m & \sigma_{y2b} &= 32.6 \mu m \\
 \sigma_{z1a} &= 84.0 mm & \sigma_{z1b} &= 90.7 mm & \sigma_{z2a} &= 85.0 mm & \sigma_{z2b} &= 42.5 mm \\
 \rho_{xy1a} &= 0.16 & \rho_{xy1b} &= 0.25 & \rho_{xy2a} &= 0.26 & \rho_{xy2b} &= -0.06
 \end{aligned}$$

The simulation was created without using the correlation factors, to clearly see the "correlation" effect of the smearing procedure. As shown in previous figures, the smearing doubles the widths of the bunches and even creates correlations in the xy-plane. The histograms with 2D Gaussian fits are in Fig.6.4 and Fig.6.5. This finding will be further investigated in future research.

---

<sup>1</sup>This was a personal communication between Dr. Mayer and Dr. Contreras, my supervisor.

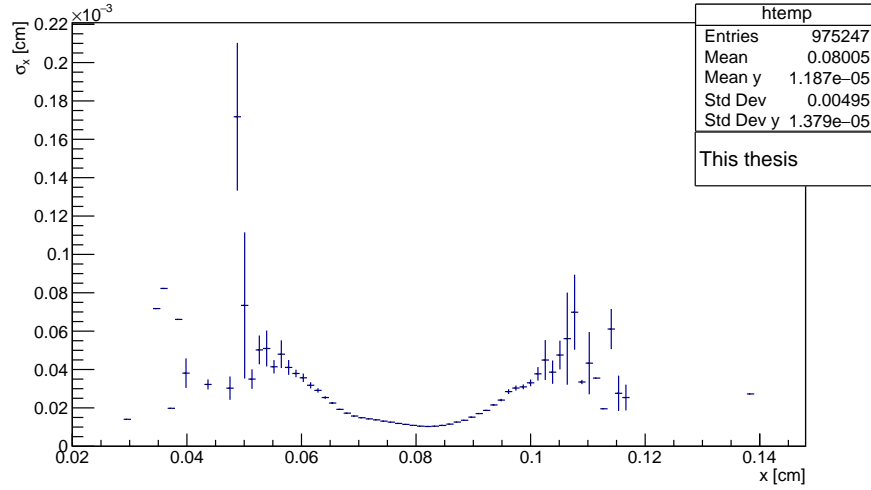


Figure 6.1: Dependence of the resolution on the vertex position in the  $x$ -direction. For the most part the resolution  $\sigma_x$  is around  $20\mu m$ , which is comparable to the bunch width.

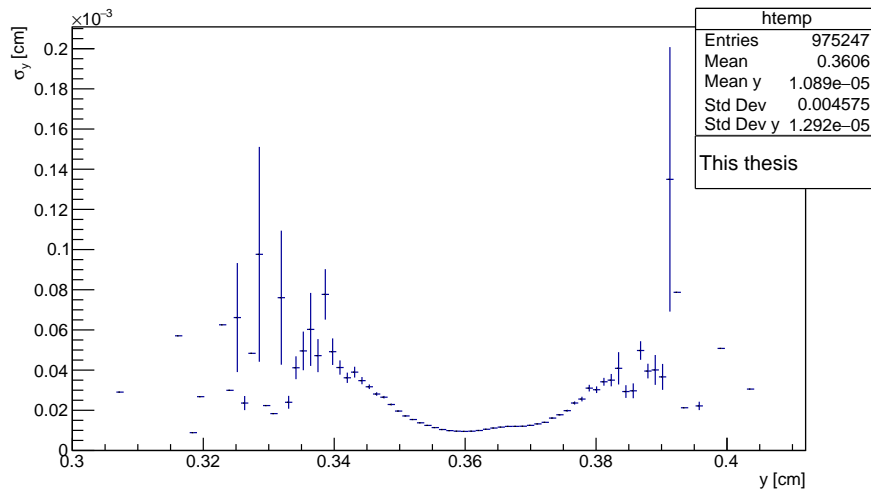


Figure 6.2: Dependence of the resolution on the vertex position in the  $y$ -direction. For the most part the resolution  $\sigma_y$  is around  $20\mu m$ , which is comparable to the bunch width.

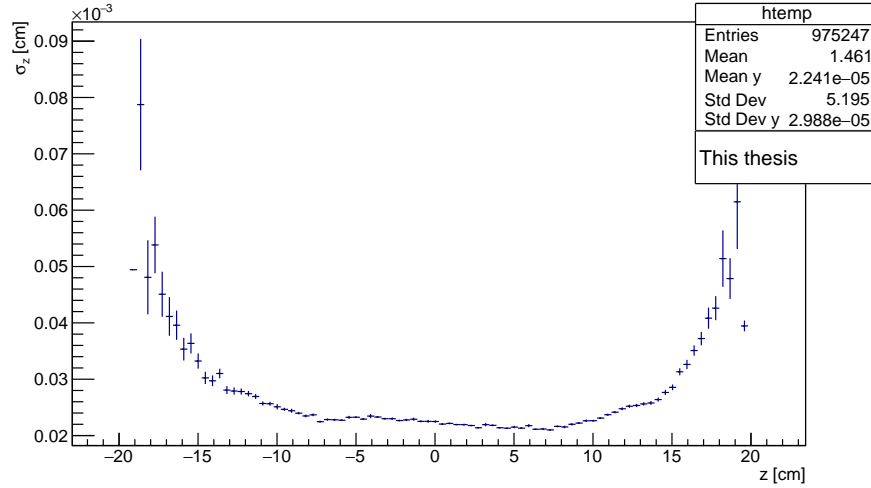


Figure 6.3: Dependence of the resolution on the vertex position in the  $z$ -direction. For the most part the resolution  $\sigma_x$  is around  $30\mu m$ , which is three orders of magnitude smaller than the bunch width.

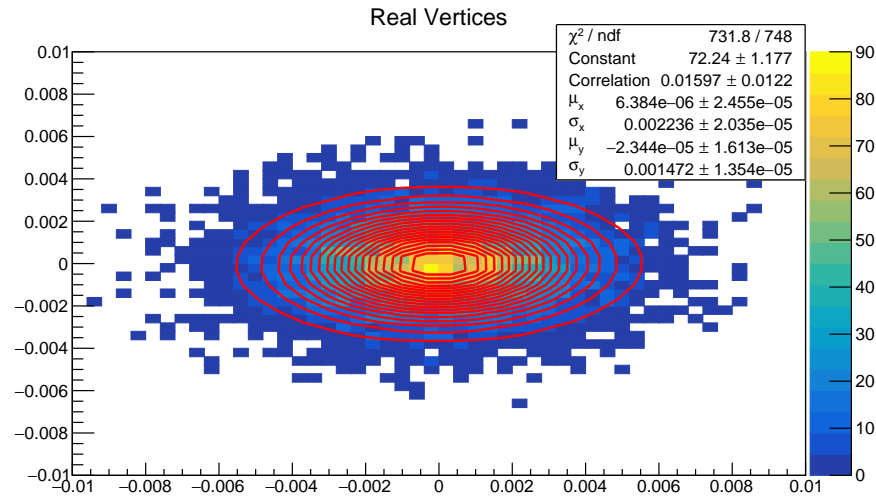


Figure 6.4: Histogram of generated vertices before smearing, fitted by a 2D Gaussian. The obtained correlation is one fit error away from 0, which is not considered conclusive.

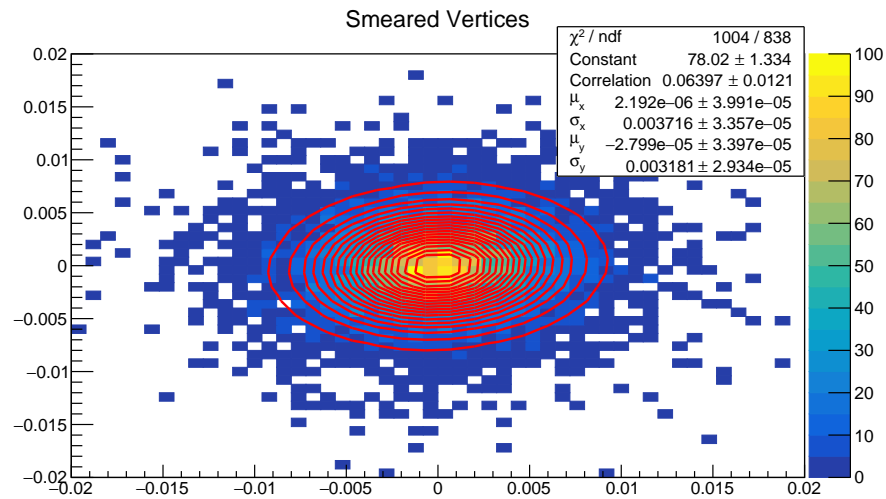


Figure 6.5: Histogram of smeared vertices from Fig.6.4. The axes have a different scale. The fit output indicates a non-zero correlation factor. This result confirms the need for further research.

## Chapter 7

# Conclusion

The luminosity formalism has been presented together with the method used at the LHC to calibrate luminometers – the van der Meer scan. Four LHC experiments were described with the focus on actual execution of the method. Also several other methods were briefly introduced (Beam-Gas Imaging, Pixel Cluster Counting etc.). During the simulation benchmarking the uncertainty was computed to be 0.5%, by comparing results with analytical predictions. The benchmark included an examination of offset collisions, collisions under a crossing angle and by combining both – collisions with a crossing angle and an offset. The obtained uncertainty was used to estimate the uncertainty of the luminosity determination using Double Gaussian bunches with a very close match to the expected uncertainty of 0.25%.

The last part of Chapter 5 was dedicated to bunch non-factorisation, which can bias the measured luminosity. For this reason a ratio  $R$  is established, which formulates the ratio between the true luminosity to the one measured by the vdM method. This phenomenon is simulated and compared to analytical results – see Fig.5.10.

The above did not account for detector effects, which possibly could change the observables. To get an insight, the simulation used real data to create detector smearing. The smeared data were fitted and compared to a fit of generated (non-smeared) data. The comparison pointed out a "creation" of correlation in the smeared luminosity region (correlation factor =  $0.06 \pm 0.01$ ).

There are few more items to study in this research project such as – the non-factorisation ratio for Double Gaussian bunches, compared to analytical predictions. It would be desirable to study the effect of the crossing angle on the non-factorisation ratio. It is needed to further examine the generated vertices by using several fit models (3D Gaussian, 3D Double Gaussian etc.) and understand the uncertainties which arise from using an inappropriate fit model. To develop an "unfolding" method would be very beneficial as well.

# Bibliography

- [1] Gabriel Anders. *Absolute luminosity determination for the ATLAS experiment*. PhD thesis, CERN, 2013. URL: [http://inspirehep.net/record/1296442/files/525947540\\_CERN-THESIS-2013-111.pdf](http://inspirehep.net/record/1296442/files/525947540_CERN-THESIS-2013-111.pdf).
- [2] Tai Sakuma. 3D SketchUp images of the CMS detector (120918). May 2016. URL: <https://cds.cern.ch/record/2628527>.
- [3] Arturo Tauro. ALICE Schematics. General Photo, May 2017. URL: <http://cds.cern.ch/record/2263642>.
- [4] Joao Pequena. Computer generated image of the whole ATLAS detector. Mar 2008. URL: <http://cds.cern.ch/record/1095924>.
- [5] Rolf Lindner. LHCb layout\_2. LHCb schema\_2. LHCb Collection., Feb 2008. URL: <https://cds.cern.ch/record/1087860>.
- [6] Jan Pucek. Stanovení luminozity v experimentu ALICE. Bachelor's Thesis, FNSPE, 2017.
- [7] Mikhail Zobov. Crab Waist collision scheme: a novel approach for particle colliders. *J. Phys. Conf. Ser.*, 747(1):012090, 2016. arXiv:1608.06150, doi:10.1088/1742-6596/747/1/012090.
- [8] R. B. Palmer. Energy Scaling, Crab Crossing, and the Pair Problem. *eConf*, C8806271:613–619, 1988.
- [9] Rama Calaga, Ofelia Capatina, and Giovanna Vandoni. The SPS Tests of the HL-LHC Crab Cavities. In *Proceedings, 9th International Particle Accelerator Conference (IPAC 2018): Vancouver, BC Canada*, page TU-PAF057, 2018. doi:10.18429/JACoW-IPAC2018-TUPAF057.
- [10] S. van der Meer. Calibration of the Effective Beam Height in the ISR. 1968.
- [11] C. Rubbia. Measurement of the Luminosity of p anti-p Collider with a (Generalized) Van Der Meer Method. 1977.
- [12] Roel Aaij et al. Precision luminosity measurements at LHCb. *JINST*, 9(12):P12005, 2014. arXiv:1410.0149, doi:10.1088/1748-0221/9/12/P12005.

- [13] P Odier, M Ludwig, and S Thoulet. The DCCT for the LHC Beam Intensity Measurement. Technical Report CERN-BE-2009-019, CERN, Geneva, May 2009. URL: <https://cds.cern.ch/record/1183400>.
- [14] D Belohrad, O R Jones, M Ludwig, J J Savioz, and S Thoulet. Implementation of the Electronics Chain for the Bunch by Bunch Intensity Measurement Devices for the LHC. Technical Report CERN-BE-2009-018, CERN, Geneva, May 2009. URL: <https://cds.cern.ch/record/1183399>.
- [15] Fabienne Marcastel. CMS brochure (English version). Brochure CMS (version anglaise). Jul 2014. URL: <https://cds.cern.ch/record/1966126>.
- [16] CMS luminosity measurement for the 2015 data-taking period. Technical Report CMS-PAS-LUM-15-001, CERN, Geneva, 2017. URL: <https://cds.cern.ch/record/2138682>.
- [17] Emittance scans for CMS luminosity calibration in 2017. Feb 2018. URL: <https://cds.cern.ch/record/2306378>.
- [18] Fabienne Marcastel. ALICE brochure (English version). Brochure ALICE (version anglaise). Jul 2014. URL: <https://cds.cern.ch/record/1965941>.
- [19] Betty Bezverkhny Abelev et al. Measurement of visible cross sections in proton-lead collisions at  $\sqrt{s_{NN}} = 5.02$  TeV in van der Meer scans with the ALICE detector. *JINST*, 9(11):P11003, 2014. arXiv:1405.1849, doi:10.1088/1748-0221/9/11/P11003.
- [20] Christiane Lefevre. ATLAS Brochure (English version). Brochure d'ATLAS (version anglaise). Oct 2011. URL: <https://cds.cern.ch/record/1426673>.
- [21] M. Aaboud et al. Luminosity determination in pp collisions at  $\sqrt{s} = 8$  TeV using the ATLAS detector at the LHC. *The European Physical Journal C*, 76(12):653, Nov 2016. URL: <https://doi.org/10.1140/epjc/s10052-016-4466-1>, doi:10.1140/epjc/s10052-016-4466-1.
- [22] Fabienne Marcastel. LHCb brochure (English version). Brochure LHCb (version anglaise). May 2014. URL: <https://cds.cern.ch/record/1965985>.
- [23] R. Brun and F. Rademakers. ROOT: An object oriented data analysis framework. *Nucl. Instrum. Meth.*, A389:81–86, 1997. doi:10.1016/S0168-9002(97)00048-X.
- [24] Betty Bezverkhny Abelev et al. Performance of the ALICE Experiment at the CERN LHC. *Int. J. Mod. Phys.*, A29:1430044, 2014. arXiv:1402.4476, doi:10.1142/S0217751X14300440.